ELSEVIER

Surface Science 458 (2000) 80–90

surface science

www.elsevier.nl/locate/susc

Oxidation of a polycrystalline titanium surface by oxygen and water

Gang Lu, Steven L. Bernasek *, Jeffrey Schwartz

Department of Chemistry, Princeton University, Princeton, NJ 08544-1009, USA

Received 21 October 1999; accepted for publication 26 January 2000

Abstract

Reactions of a well-characterized polycrystalline titanium surface with oxygen and water molecules at 150–850 K were studied in UHV by X-ray photoelectron spectroscopy (XPS), thermal desorption spectroscopy (TDS) and Fourier transform reflectance–absorption infrared spectroscopy (FT-RAIRS). At 150 K, O_2 oxidizes Ti^0 to Ti^{IV}, Ti^{III} and Ti^{II}, but Ti exposure to H_2O at this temperature produces only Ti^{II} species. At temperatures above 300 K, further oxidation of Ti by H_2O was observed. Maximum oxidation by either molecule is achieved at 550–600 K. Upon heating the oxidized titanium above 850 K, the oxide layer is completely reduced to Ti^0. Hydroxyl species are identified on the Ti surface after reaction with H_2O; they appear to be mostly hydrogen bonded between 250 and 350 K, and isolated in the 450–650 K surface temperature range. Depth profiling of the O_2-oxidized Ti surface shows that Ti^{IV}/Ti^{III} species account for about 20% of the total thickness of the oxide layers and are located near the surface, while Ti^{II} has a broader distribution, and is concentrated close to the oxide–metal interface. The OH group concentration is maximized at 550 K on the sample surface and accounts for about 16% of the total surface oxygen, with a decreasing concentration of OH into the bulk of the titanium oxides.

Keywords: Chemisorption; Oxidation; Oxygen; Thermal desorption spectroscopy; Titanium; Titanium oxide; Water; X-ray photoelectron spectroscopy

1. Introduction

Surface modification of metals has potentially practical applications in corrosion inhibition [1], heterogeneous catalysis [2], sensors [3], electrochemistry [4] and medical devices [5]. Except for a few noble metals, all transition metals are covered with native oxide as well as hydroxyl layers; this oxide/hydroxide 'native' coating can be an obstacle to controlled surface modification by formation of strong metal–organic interfaces (such as the difficulty in producing stable self-assembled monolayers with alkanethiols on metals other than gold). This native oxide hydroxylated coating can also be exploited for developing covalent metal–organic bonds for surface modification, through organometallic interfaces [6–12]. Indeed, details of transition metal surface modification via reaction of oxide/hydroxide with organic and organometallic compounds have been studied both in this laboratory [6–17] and elsewhere [18–25] for a number of years.

Titanium metal combines the strength of iron and steel with the light weight of aluminum, which accounts for its widespread use in the aviation and

* Corresponding author. Fax: +1-609-258-1593.
E-mail address: sberna@princeton.edu (S.L. Bernasek)

0039-6028/00/$ - see front matter
PII: S0039-6028(00)00420-9

aerospace industries, in high performance sports equipment, and in the medical field for bone implants and replacement devices [26]. Understanding and controlling surface modification of titanium is necessary for optimization of these applications and developing new ones. For example, the formation of reliable and reproducible organic coatings on the titanium native oxide/hydroxide surface requires a knowledge of both oxidation and hydroxylation processes. In order to maximize covalent bonding of organometallic compounds with the native oxidized titanium surface, a high coverage of surface OH groups is required, and the thermal characteristics of the native oxide and hydroxyl layers might be directly correlated with the stability of the functional organic overlayers that are synthesized upon them. Most detailed surface science studies related to titanium have focused on the surface of bulk oxide TiO_2, owing to its importance in heterogeneous catalysis [27] and photocatalysis [28]. Much less attention has been directed to the formation of the native oxide layers on the titanium metal surface itself, and in particular the formation of hydroxyl groups, which are very important for titanium surface modification via an organometallic interface. In addition, little is known about the quantitative composition of the oxide/hydroxide overlayer that forms on titanium metal, the basic mechanism of the overlayer formation, or the detailed conditions leading to a particular oxide/hydroxide overlayer composition.

In previous work, surface Ti^{II}, Ti^{III} and Ti^{IV} species have been identified [29] following reaction of the metal with dioxygen. Angle-dependent XPS was used to demonstrate qualitatively that titanium species of high oxidation state are located furthest from the metal, and those of lower oxidation state are, for the most part, close to the oxide–metal interface. This qualitative information about the distribution of various titanium oxidation state oxides was supported by a thermodynamic analysis [30]. Oxygen, NO, and CO have been used to oxidize titanium to a range of oxidation states (4+, 3+ and 2+, respectively) under similar temperature and pressure conditions [31]. The oxidation of titanium films vapor deposited on a metal substrate has been studied before using a quartz crystal microbalance (QCM) [32] and Auger electron spectroscopy (AES) [33]. It is generally agreed that Ti oxidation is characterized by fast oxygen adsorption, followed by slower oxygen uptake until saturation is reached. Titanium dioxide films on Mo(100) have been prepared by evaporating Ti in an atmosphere of O_2, and the film has been characterized by ion scattering (ISS), XPS and low energy electron diffraction (LEED) [34]. It was found that TiO_2 growth is epitaxial; after annealing to 900–1200 K, the films are partially reduced and exhibit both Ti^{III} and Ti^{II} oxidation states. Water reactions with polycrystalline titanium have been studied using photocurrent measurement [35] at 1123 K, which showed that the oxidation of Ti by water vapor is faster than that by oxygen. However, as determined by direct recoil spectrometry (DRS), AES and XPS, the oxidation efficiency of water at 300 K seems to be much lower than that of oxygen [36]. This reduced oxidation efficiency was attributed to the presence of hydroxyl species. Clearly, a systematic study of the oxidation and hydroxylation behavior of the titanium surface is warranted as a first step toward quantifying the oxide/hydroxide overlayer on titanium. This information will be very useful in understanding and developing titanium surface modification chemistry. In this paper, XPS, TDS and FT-RAIRS investigations of a well-characterized polycrystalline titanium surface in its reactions with molecular oxygen and water in the temperature range of 150–900 K in UHV are reported. Exposure and temperature dependence of titanium oxidation by these two species have been characterized, and three-dimensional spatial distributions of both hydroxyl groups and various oxides have been quantitatively examined by depth profiling and electron spectroscopy techniques.

2. Experimental

The UHV chamber used for this work has been described previously [37]. A Varian V-550 turbomolecular pump enables a base pressure of 2×10^{-10} Torr to be maintained routinely. Because of high pumping speed, the base pressure in the

chamber can be maintained at 5×10^{-10} Torr, even after cycles of substrate water dosing. The chamber is equipped with a quadrupole mass spectrometer (UTI-100C), and facilities for Fourier transform reflectance–absorption infrared spectroscopy (Mattson RS-1) and X-ray photoelectron spectroscopy (Perkin-Elmer).

A titanium polycrystalline foil (1 mm thick; Goodfellow Corp.) had nominal purity of 99.999%, and H content about 4 ppm [38]. It was cut into a square 18 mm × 18 mm and polished on one side using fine Al_2O_3 powders from 5 to 0.05 μm. After repeated ultrasonic cleaning, first with toluene and then acetone, the sample was mounted onto a button heater (Heatwave) with tungsten wires to hold tight the sample corners. A chromel–alumel thermocouple was spot welded at the front edge of the sample. The Ti surface was cleaned through cycles of Ar^+ ion bombardment ($22\ A\ cm^{-2}$) and annealing to 850 K, until no oxygen and carbon were detected by XPS. Lower Ar^+ ion flux ($10\ A\ cm^{-2}$) was used for the XPS depth profiling. Gas dosing was facilitated through a carefully cleaned gas manifold. Both O_2 and H_2O vapor were directed onto the sample surface through two separate gas lines and leak valves using internal stainless steel tubes (diameter = 6.4 mm) with their openings about 20 mm away from the sample surface. Gas exposures were calculated from uncorrected ion gauge reading; the real exposure at the sample may be one or two orders of magnitude higher [39]. Ultradry O_2 gas (Matheson) showed no detectable contamination, by mass spectrometry. In particular, no increase in water partial pressure (ca. 10^{-11} Torr) was observed during O_2 dosing. Deionized water was used after degassing by multiple freeze-and-thaw cycles.

XPS data analysis was accomplished using a Shirley background [40] for the clean titanium and a mixed linear and Shirley background for the oxidized titanium sample. The line shape of the XPS spectra used was a mixed Gaussian–Lorentzian sum function, with the optimal mixing ratio obtained from the best fitting of standard samples of Ti metal and TiO_2; this mixing ratio was used for the entire data analysis. Asymmetrical line shapes were used for Ti^0, and symmetrical ones for the oxidized Ti components, as well as for O 1s. Binding energies are all calibrated against Ti^0 (BE[Ti $2p_{3/2}$] = 454.1 eV) [41]. To enhance the reliability of the curve fitting procedures used to analyze the mixed oxidation state layers observed here, the number of fitting parameters has been reduced as much as possible. For example, the peak positions of the four species in a Ti 2p spectral analysis were always fixed to the literature values. Their Gaussian/Lorentzian mix ratios, $p_{1/2}$ and $p_{3/2}$ peak area ratio (1:2) and the $p_{1/2}$ to $p_{3/2}$ peak splitting (6.17 eV in Ti and 5.54 eV in TiO_2) were all fixed, and the peak widths are constrained within a range. This allows only the peak areas to change freely in the fit, greatly reducing any ambiguity in the data analysis. The peak areas versus sputtering time data collected in the XPS depth profiling work was converted to atomic concentration versus sputtering time taking into account the relatively large XPS probing depth [42].

3. Results

3.1. Oxidation by O_2

Ti 2p XPS spectra of a clean Ti surface and after cycles of O_2 dose at 650 K were recorded (Fig. 1). Each dose was an exposure of 6 L followed by turning off the heating and closing the O_2 leak valve. The last spectrum (Fig. 1f) shows the oxidized sample after heating to 850 K for 1 min in vacuum. Surface oxidation was immediately observed with the first cycles of O_2 exposure. The complicated Ti 2p profile (Fig. 1b) can be deconvoluted into four Ti 2p components, based on published binding energies of 458.8, 457.5, 455.1 and 454.1 eV for TiO_2, Ti_2O_3, TiO and Ti, respectively [29,43,44]. The apparent relative intensities of the oxides are in the order of $TiO_2 > Ti_2O_3 > TiO$. Owing to the preferential distribution of the TiO_2 species at the outer surface layer and suboxides closer to the metal inner layers (see later) and the attenuation of photoelectrons from the deeper layers, this intensity ratio may not reflect the absolute quantitative amount of the oxides. However, relative changes in titanium

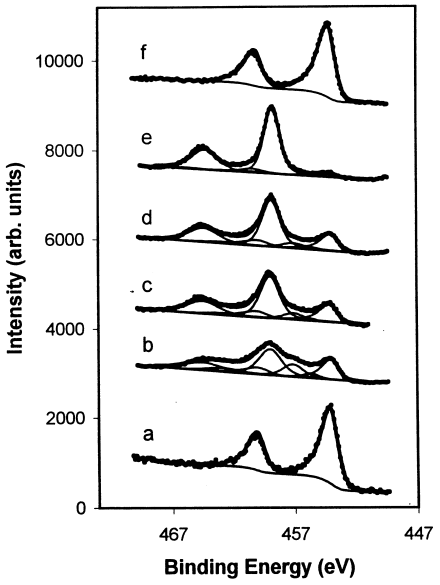

Fig. 1. Ti 2p XPS spectra of a clean Ti sample (a) at 650 K, and after exposures to O_2 of (b) 6 L, (c) 12 L, (d) 18 L, (e) 24 L, and finally heating to 850 K (f) in vacuum.

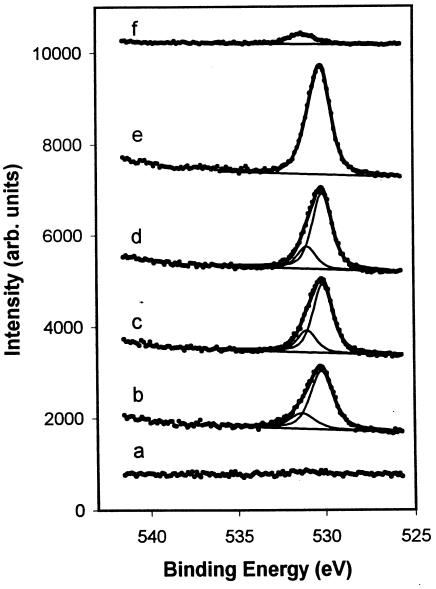

Fig. 2. O 1s XPS spectra of a clean Ti sample (a) at 650 K, and following exposures to O_2 of (b) 6 L, (c) 12 L, (d) 18 L, (e) 24 L, and finally heating to 850 K (f) in vacuum.

oxide distribution as a function of exposure (Fig. 1b–e) are obvious: the TiO_2 layer thickens and the spectral intensity due to the suboxides and Ti^0 decreases with increasing O_2 exposure. When the heavily oxidized Ti sample is heated above 850 K in vacuum for 1 min, the TiO_2 and Ti_2O_3 components disappear; the sample surface only shows Ti^0 and a small amount of TiO (Fig. 1f).

O 1s XP data (Fig. 2) complement those for Ti 2p. With one cycle of 6 L O_2 dose, an asymmetrical peak is observed in the O 1s region (Fig. 2b). This profile can be properly fit with two symmetrical peaks, one at 530.1 eV and another at 531.2 eV. The main O 1s peak is certainly associated with TiO_2 and perhaps Ti_2O_3, the dominant components in Fig. 1b. (The O_{1s} binding energy of TiO_2 has been reported to be 529.9 eV [31]). The minor peak at higher binding energy is likely due to TiO. As the O_2 exposure increases, two observations are remarkable: the asymmetry of the O 1s peak gradually diminishes, and the area of the main peak increases, while that of the minor peak decreases (Fig. 2b–e). The binding energy of the O 1s peak in Fig. 2e at 530.1 eV is assigned to TiO_2, which agrees well with the Ti 2p results. After the sample is flash heated to 850 K, only a small O 1s peak ($\sim$10% of the original area) remains at 531.2 eV, in good agreement with the Ti 2p observations that TiO is the only oxide species on the surface at this temperature. Mass spectrometry was used to follow the thermal reduction process. No Ti-containing species were observed; the only detected positive ion was O^+. Surprisingly, no thermal desorption of O_2 species was detected. Desorption of O was prominent and peaked at 800 K, consistent with XPS observation that above 850 K virtually all oxygen was gone from the O_2/Ti substrate.

The titanium oxidation depth and the oxide distributions formed depend not only on the O_2 exposure, but more importantly on the sample temperature. To investigate this temperature dependence, a fixed amount of O_2 (3 L) was dosed onto a clean Ti surface, and the temperature was increased stepwise from 150 to 850 K with each O_2 exposure. Variations in the Ti 2p and O 1s peak areas of all the titanium oxide species (Ti^0 to Ti^{IV}) were measured with the changing temperature (Figs. 3 and 4). At 150 K, the reaction of O_2 with

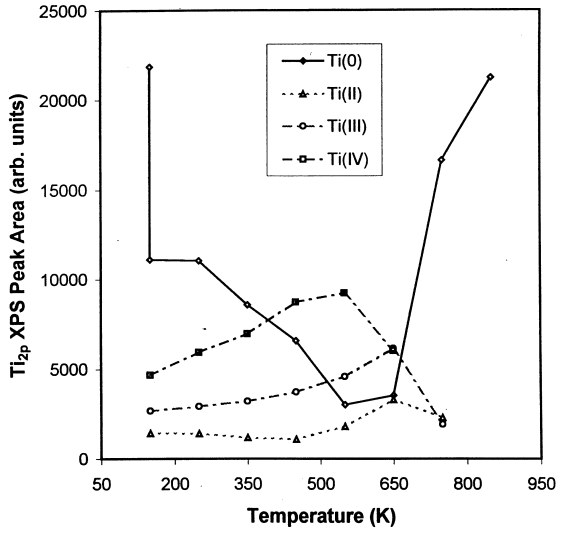

Fig. 3. Variation of the Ti 2p peak area with the sample temperature for Ti^0, Ti^{II}, Ti^{III} and Ti^{IV} in a temperature-dependent oxidation of the Ti surface with 3 L O_2.

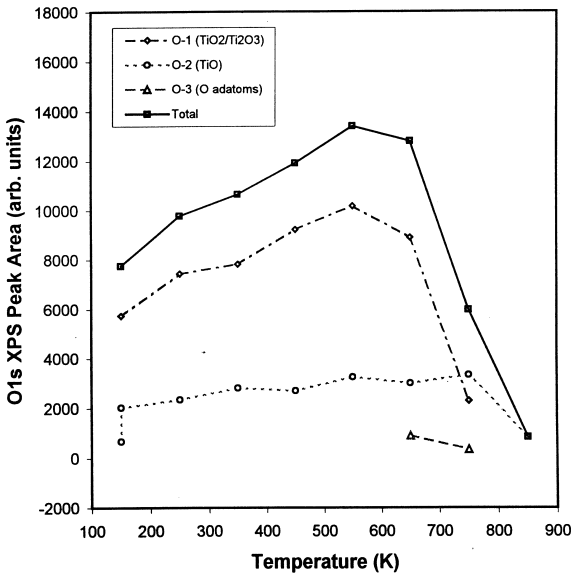

Fig. 4. Variation of O 1s peak area with the sample temperature for the total oxygen and its three components: O-1 (TiO_2/Ti_2O_3), O-2 (TiO) and O-3 (O radical) in a temperature-dependent oxidation of the Ti surface with 3 L O_2.

Ti produces a full range of titanium oxides (Fig. 3). As the sample temperature increases, the Ti^0 intensity decreases and reaches a minimum at around 550–650 K, while that for the titanium oxides shows an opposite trend. The intensity for Ti^{IV} species maximized at 550 K and for Ti^{II} and Ti^{III} at 650 K. In the temperature range of 150–650 K, O_2 dissociation at the Ti surface and diffusion into the bulk is the dominant process. Above 650 K, all titanium oxides are reduced in quantity. In this temperature range, the diffusion of oxygen from the bulk and desorption are the overriding processes; ultimately all oxygen is desorbed from the Ti substrate above 850 K, and the Ti^0 peak intensity returns to its starting value.

Plots of O 1s XPS data versus temperature (Fig. 4) show the same trends observed for Ti 2p (Fig. 3). Nearly coincident with profiles for Ti^{III} and Ti^{IV} is the steady growth of the main oxygen peak (O-1) in the temperature range 150–600 K and the rapid loss in intensity for this species at higher temperature. Similarly, the small peak (O-2) at 1.2 eV higher binding energy than the main peak shows a very weak temperature dependence, as does the behavior of the Ti^{II} species (Fig. 3). Therefore, (O-1) is likely the oxygen present in TiO_2 and Ti_2O_3, and O-2 is the oxygen of TiO. By carefully examining the profiles of the O 1s XPS spectra of 650 and 750 K, a third peak (O-3) at binding energy 3.1 eV higher than that of the main peak, is apparent. Considering its high binding energy and its appearance at a temperature where oxygen diffusion from the bulk and desorption of oxygen into the vacuum is likely, this peak may be assigned as an oxygen radical at the surface [45].

3.2. Reaction with H_2O

Water reactions with a clean Ti surface were effected with cycles of H_2O dosing at 150 K followed by warming to 300 K, and also by H_2O dosing at 300 K. In both cases no titanium oxide species higher than TiO is observed by XPS. FT-RAIRS analysis of the water reaction shows a broad band centered at 3450 cm^{-1} and a small band at 1700 cm^{-1} following a 5 L H_2O dose at 150 K. The intensities of both bands increase and the broad band shifts to 3250 cm^{-1} when H_2O exposure is increased. This indicates multilayer molecular water condensation onto the sample surface. The IR spectra shows decreasing inten-

sities for both bands upon slowly warming. Above 190 K all bands in the IR disappear even though XPS shows clear evidence of oxidation and OH formation above this temperature. This is likely to be a result of the dramatic change in IR background in going from the clean Ti to the TiO substrate, preventing the observation of the IR spectra.

Multilayer water formation at 150 K was also monitored in the O 1s XPS peak at 2.9 eV higher binding energy than that of the peak for TiO. Warming the sample to 300 K showed no shoulder characteristic of the OH species. Repeated water doses at 300 K were carried out. The O 1s peak intensity increased rapidly after one dose of 2.4 L and the O 1s peak appeared to saturate with a 16% increase in intensity after three further H_2O doses, for a total of 14.7 L.

The surface and subsurface H_2O and OH concentrations on a Ti sample exposed to H_2O vapor were affected greatly by substrate temperature. Thermal desorption profiles of H_2O from Ti were obtained from samples prepared at various H_2O deposition temperatures. When H_2O was dosed at 150 K, four molecular water desorption peaks were observed: multilayer H_2O at 160–200 K; chemisorbed molecular H_2O at around 450 K; water likely from surface hydroxyl group recombination, at ca. 670 K; and a higher temperature desorption at 750–800 K, which may be due to recombination of subsurface OH. Water reaction with Ti at 250 K showed a different TDS profile. The overall area under the profile was much smaller than for reaction at 150 K, partly because of the smaller water sticking coefficient. The multilayer H_2O peak was gone, as was chemisorbed molecular H_2O. The OH recombination peaks were reduced in intensity, and the subsurface OH recombination peak was shifted to 880 K, indicating higher temperatures are needed to drive recombination of OH located more deeply in the bulk out to the surface. Similar changes are also observed in the 350–550 K profiles, with an additional change in the surface OH recombination peak. In this case a large portion of the peak component around 670 K disappeared, leaving a portion of the original peak at 710 K. The 670 K component is assigned as recombination from the hydrogen-bonded OH species, and the 710 K peak as recombination of the isolated OH species. Once the Ti temperature was raised to 850 K, for initial water exposure, no desorption of any species was observed above 300 K. Weak $m/e=17$ desorption profiles in addition to H_2O were also recorded, from 150 to 750 K. Owing to the similarity in shape for these two species, $m/e=17$ is likely a fragment of H_2O produced in the mass spectrometer, and not a direct OH desorption product. No O_2 nor any Ti-containing species were detected during the TDS.

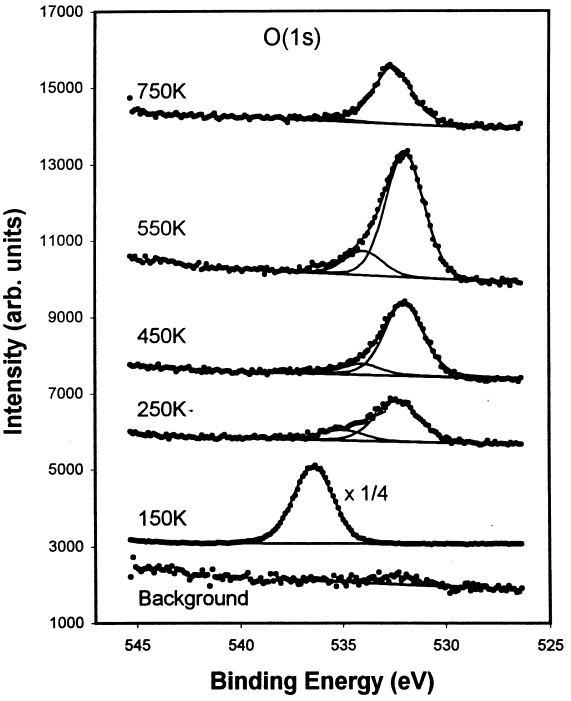

Fig. 5. O 1s XPS spectra of the clean Ti surface reaction with 6 L H_2O at the sample temperatures of 150–850 K.

O 1s XPS spectra of temperature-dependent H_2O deposition on Ti were recorded (Fig. 5). To make a stoichiometrically quantitative comparison with results from the O_2 reaction with Ti, 6 L H_2O exposure was effected at each sample temperature from 150 to 850 K. A very intense O 1s peak, due to molecular H_2O, was observed at 150 K, while the substrate Ti 2p signal was totally screened by the thick ice layer. At 250 K, the

titanium surface was oxidized by H_2O to TiO, and a hydrogen-bonded OH species was seen as a shoulder, at a binding energy 2.7 eV higher than that of the O 1s peak of TiO. Starting at 450 K, Ti_2O_3 and TiO_2 species were formed along with TiO; isolated hydroxyl group formation during the reaction is evident by the small side peak 1.5 eV above the oxide oxygen peaks. Maximum hydroxylation was achieved at 550 K. Higher sample temperatures lead to the diminution of the hydroxyl peak (650 K), and finally the total loss of OH and reduction of oxide oxygen (>750 K).

3.3. Depth profiling

The apparent peak intensities for the three titanium species present as oxides are in the order: $Ti^{IV} > Ti^{III} > Ti^{II}$. It is well known that for a fixed XPS experimental geometry, peak intensity is determined not only by the atomic concentration of an element, but also by the depth distribution of the element in the sample [42]. Using angle-resolved XPS, Carley [29] concluded for the O_2/Ti system that, qualitatively, Ti^{IV} and Ti^{III} are located predominantly at the sample–vacuum interface, and that Ti^{II} resides chiefly near the oxide–Ti^0 interface. In general, the present depth profiling study of the O_2/Ti system agrees with this result. The depth profiling data also show quantitatively the distribution of the three oxides in the sample surface region. Changes in the Ti 2p XPS spectra of the Ti surface sputtered by Ar^+ ions over a period of 90 min were measured (Fig. 6). As the mixed Ti oxide layer (formed by 3 L O_2 deposition at 550 K) was gradually removed with continuing Ar^+ ion bombardment, the O 1s region XPS also showed a progressive increase of the oxygen attributed to Ti<u>O</u>, at the expense of the oxygens of Ti<u>O</u>$_2$ and Ti_2<u>O</u>$_3$. Indeed, coincident with the removal of TiO_2 and Ti_2O_3 from the surface, the asymmetry of the O 1s peak disappeared and, finally, it could be fit with a single, symmetric peak, characteristic of TiO.

Quantitative variation in atomic concentration of the four Ti species with sputtering time is shown in Fig. 7. The Ti^{IV} and Ti^{III} layers are thin and

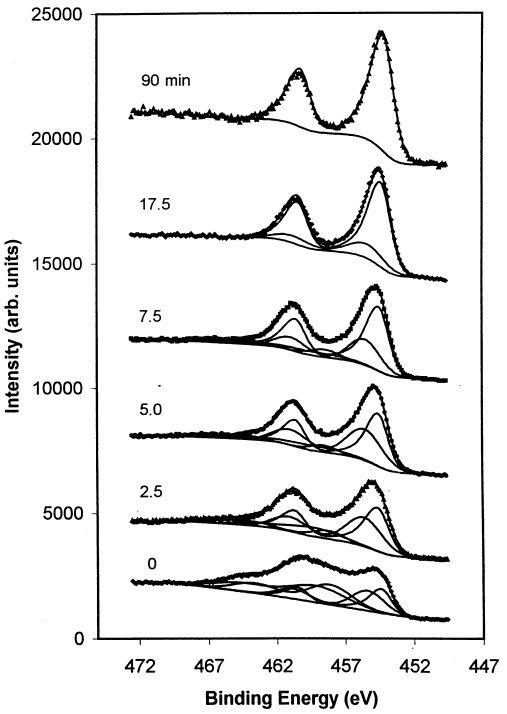

Fig. 6. Representative Ti 2p XPS spectra of an oxygen-oxidized Ti surface (3 L, 550 K), undergoing Ar^+ ion sputtering for 90 min.

located primarily near the topmost sample surface; Ar^+ sputtering showed rapidly reduced concentrations for these oxidation states of the metal inside the bulk. The overall Ti^{IV}–Ti^{III} layer accounts for 20% of the total thickness of the oxide layers. No Ti^0 was detected in this region. The low concentration of Ti^{II} observed at the surface may be due to the partial reduction of higher oxides to lower oxides during sputtering: Ar^+ ion sputtering is known to preferentially remove O atoms from the TiO_2 surface [46]. Below the Ti^{IV}–Ti^{III} layers, Ti^{II} coexists with Ti^0; the Ti^{II} concentration gradually drops to zero with continued sputtering.

Depth profiling H_2O-oxidized Ti provides information on the distribution of not only mixed Ti oxides, but more importantly on the distribution of OH species on and beneath the sample surface. Depth profiles with stepwise Ar^+ ion sputtering, elucidating the concentrations of OH, TiO and Ti_2O_3/TiO_2 species in a Ti sample oxidized by 6 L of H_2O at 550 K, are shown in Fig. 8. The O 1s

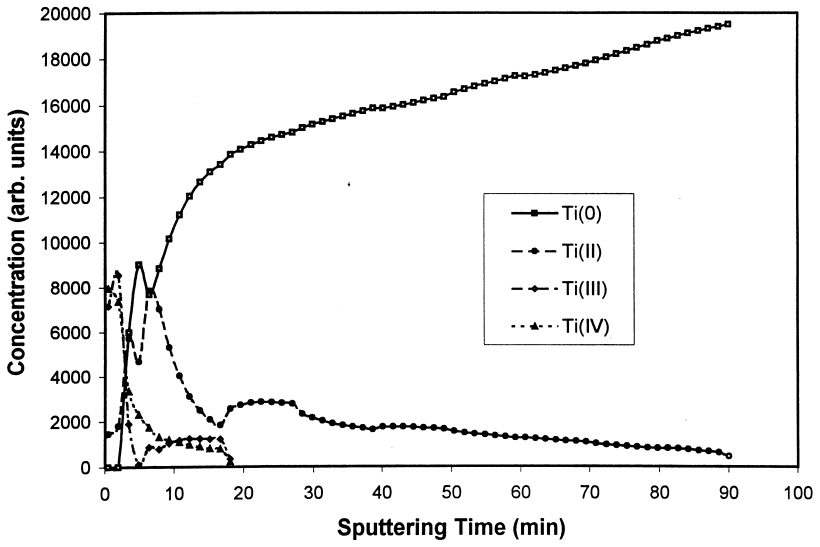

Fig. 7. Variations of the concentration of Ti^{0}, Ti^{II}, Ti^{III} and Ti^{IV} species with Ar^{+} ion sputtering time for a Ti surface exposed to 3 L O_2 at 550 K.

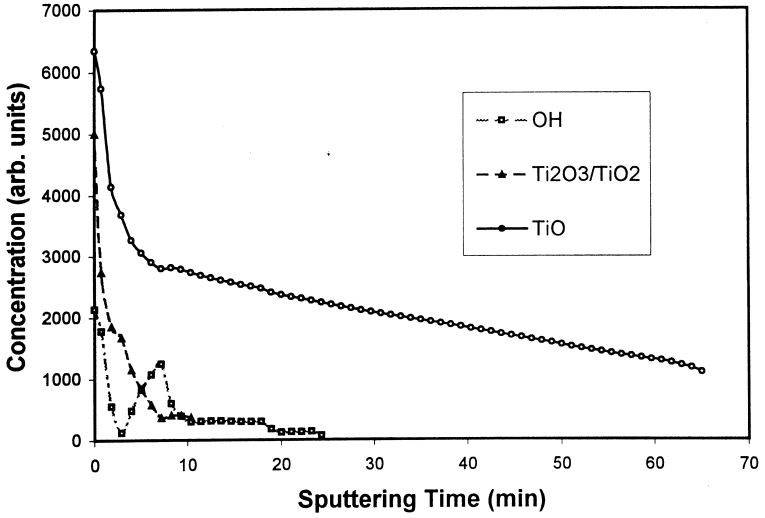

Fig. 8. Variations of the concentration of OH, TiO and Ti_2O_3/TiO_2 species with Ar^{+} ion sputtering time for a Ti surface exposed to 6 L of H_2O at 550 K.

XPS cannot completely differentiate the oxygen in Ti_2O_3 and TiO_2, so the combined data are displayed. Contrary to the case of O_2/Ti, the most abundant oxide species at the surface is TiO, followed by a smaller amount of Ti_2O_3/TiO_2. Based on the Ti XPS data, the ratio of Ti^{IV} to Ti^{III} is 1:1, thus the relative surface concentration of TiO to Ti_2O_3/TiO_2 is 2.1:1. The amount of OH at the surface accounts for about 16% of the total surface oxygen; the rest is oxide. Hydroxylation is highest at the surface, with a rapidly decreasing concentration of OH beneath the surface layer.

4. Discussion

The thickness of the oxide coating on Ti depends on both the duration of O_2 exposure and on the sample temperature. Raising the temperature promotes the diffusion of oxygen into the bulk of the sample, increasing overall oxidation. However, at very high temperature O atoms desorb from the surface with concomitant reduction of the Ti oxidation state. These two opposing trends indicate an optimal temperature for maximum oxidation; temperature-dependent experiments reveal this temperature to be in the range of 500–600 K.

The degree of asymmetry in the lineshapes of O 1s XPS spectra (Fig. 2) decreases as the O_2 exposure increases. This is shown by the evolution of the small higher BE peak (531.2 eV) fitted with the main symmetric peak (530.1 eV) (Fig. 2b), to the almost symmetrical, single peak of Fig. 2e. The asymmetry in the O 1s XPS spectra for Ti oxidation has been previously noted, but was either not discussed [44], or not appropriately interpreted [43]. Zanoni [43] proposed that the high BE component might come from oxygen in Ti_2O_3, Ti hydroxides or metal alkoxides. In the current study of Ti metal oxidation by O_2, H_2O contamination has been carefully controlled; furthermore, the H content in the high purity Ti sample is only 4 ppm, too low to produce any strong OH hydroxyl component in the O 1s XPS spectrum following O_2 oxidation. Thus, this high BE peak is assigned to the oxygen in TiO, based on the following. First, the overall O 1s peak shape gradually changes from asymmetric to symmetric, consistent with increasing TiO_2 concentration and decreasing detectability of TiO with increasing exposure to O_2 (Fig. 2b–e). Second, the binding energy (531.2 eV) agrees well with that of the final oxygen residual after the sample has been heated to 850 K, which gives TiO, and it is unreasonable to assume that OH groups would survive such high thermal treatment, instead of recombining to desorb water. Finally, the depth profiling of the Ti surface oxidized by O_2 showed a shift of the main O 1s peak from 530.1 to 531.2 eV with Ar^+ ion sputtering-removal of the TiO_2 rich top layers, exposing the TiO-rich inner layers.

The thermal reduction of Ti oxides above 850 K in vacuum appears to occur through loss of O. Bulk TiO_2 is also subject to oxygen loss under similar conditions and, accordingly, surface defects are created [34,47]. However, the nearly total loss of oxygen from TiO_2 has not previously been reported. It is possible that the reversible oxidation observed in the present case is due to the presence of only a thin layer of oxides, limiting the amount of O available from deep in the bulk to replenish lost *surface* oxygen. It might also be due to a lattice structure for the thin oxide layers which is less stable than that present in the bulk. An interesting observation is that, if a crystalline TiO_2 sample with thermal defects is heated in air at high temperature, the oxygen defects can be compensated rapidly [48]. This suggests that high temperature treatment promotes the mobility of oxygen in the oxide lattice and also its diffusion in and out of the sample. As the temperature increases, the oxygen atmosphere around the titanium oxide sample will prevent the *net* loss of bulk oxygen by reoxidation of any exposed, reduced Ti sites; conversely, heating in a vacuum or under H_2 will lead to the net reduction of the oxides, through loss of the oxygen atoms.

It is known that reaction of aluminum with H_2O at 150 K oxidizes Al to Al_2O_3, and that OH species are formed during the oxidation process [37]. A similar approach does not work to create surface-bound OH groups on Ti. The extent of oxidation of Ti by water is more limited: no Ti_2O_3 or TiO_2 is detected at 300 K. Moreover, the oxide layer is thin, resulting in only a small increase of O_{1s} peak intensity after several cycles of water deposition and desorption. This difference in oxidation profile may be due to thermodynamic factors, since at more than 450 K, both Ti_2O_3 and TiO_2 are formed on Ti upon reaction with H_2O.

5. Conclusions

At 150 K O_2 can oxidize Ti to Ti^{IV}, Ti^{III} and Ti^{II}, while exposure of Ti to H_2O at this temperature only produces Ti^{II} species. At temperatures above 300 K, H_2O can further oxidize Ti^{II} to higher oxidation states. At a given temperature, Ti oxida-

tion by both O_2 and H_2O slightly increases as exposure increases. However, the extent of oxidation is greatly influenced by the sample temperature. Maximum oxidation is achieved at 550–600 K. Upon heating the oxidized Ti above 850 K, the titanium oxide layer is completely reduced to Ti^0. Depth profiling of the oxidized Ti surface reveals that the Ti^{IV} and Ti^{III} species comprise the outermost 20% of the oxide layer; the remaining oxide layer, close to the metal–oxide interface, consists of Ti^{II} and Ti^0. Hydroxyl species are identified in the sample following reaction of Ti with H_2O; these hydroxyl groups are mostly hydrogen-bonded between 250 and 350 K, and exist as isolated species at 450–650 K. The maximum total OH concentration is achieved at 550 K. The OH species concentration is highest at the oxide surface, accounting for 16% of the total surface oxygen; its concentration quickly decreases below the surface.

Acknowledgements

The authors acknowledge financial support for this work provided by the National Science Foundation and the New Jersey Center for Optoelectronic Materials.

References

[1] T. Noyata, G.W. Poling, Corrosion 35 (1979) 193.
[2] G.A. Somorjai, Chemistry in Two Dimensions: Surfaces, Cornell University Press, Ithaca, NY, 1981.
[3] X. Yang, J. Shi, S. Johnson, B. Swanson, Langmuir 14 (1998) 1505.
[4] G.K.J. Budnikov, Anal. Chem. 51 (1996) 343.
[5] A. Nanci, J.D. Wuest, L. Peru, P. Brunet, V. Sharma, S. Zalzal, M.D. McKee, J. Biomed. Mater. Res. 40 (1998) 324.
[6] Y.G. Aronoff, B. Chen, G. Lu, C. Seto, J. Schwartz, S.L. Bernasek, J. Am. Chem. Soc. 119 (1997) 259.
[7] G. Lu, K.L. Purvis, J. Schwartz, S.L. Bernasek, Langmuir 13 (1997) 5791.
[8] S.K. VanderKam, G. Lu, J. Schwartz, S.L. Bernasek, J. Am. Chem. Soc. 119 (1997) 11639.
[9] K.L. Purvis, G. Lu, J. Schwartz, S.L. Bernasek, Langmuir 14 (1998) 3720.
[10] G. Lu, J. Schwartz, S.L. Bernasek, Langmuir 14 (1998) 1532.
[11] E.S. Gawalt, G. Lu, S.L. Bernasek, J. Schwartz, Langmuir 115 (1999) 8929.
[12] K.L. Purvis, G. Lu, J. Schwartz, S.L. Bernasek, Langmuir 15 (1999) 7092.
[13] L.C. Cheng, A.B. Bocarsly, S.L. Bernasek, T.A. Ramanarayanan, Surf. Sci. 374 (1997) 357.
[14] L.C. Cheng, A.B. Bocarsly, S.L. Bernasek, T.A. Ramanarayanan, Langmuir 12 (1996) 392.
[15] W.H. Hung, S.L. Bernasek, Surf. Sci. 346 (1996) 165.
[16] L.C. Cheng, S.L. Bernasek, A.B. Bocarsly, T.A. Ramanarayanan, Chem. Mater. 7 (1995) 1807.
[17] W.H. Hung, S.L. Bernasek, Surf. Sci. 339 (1995) 272.
[18] G.M. Whitesides, J.P. Mathias, C.T. Seto, Science 254 (1991) 1312.
[19] L.H. Dubois, B.R. Zegarski, R.G. Nuzzo, J. Chem. Phys. 98 (1993) 678.
[20] L.H. Dubois, R.G. Nuzzo, Annu. Rev. Phys. Chem. 43 (1992) 437.
[21] H.G. Hong, D.D. Sackett, T.E. Mallouk, Chem. Mater. 3 (1991) 521.
[22] H.C. Yang, K. Aoki, H.-G. Hong, D.D. Sackett, M.F. Arendt, S.-L. Yau, C.M. Bell, T.E. Mallouk, J. Am. Chem. Soc. 115 (1993) 11 855.
[23] M. Fang, D.M. Kaschak, A.C. Sutorik, T.E. Mallouk, J. Am. Chem. Soc. 119 (1997) 12 184.
[24] C.B. Mao, H.D. Li, F.Z. Cui, Q.G. Feng, H. Wang, C.L.J. Ma, Mater. Chem. 8 (1998) 2795.
[25] A.N. Parikh, M.A. Schivley, E. Koo, K. Seshadri, D. Aurentz, K. Mueller, D.L. Allara, J. Am. Chem. Soc. 119 (1997) 3135.
[26] M.M. Klinger, F. Rahemtulla, C.W. Prince, L.C. Lucas, J.E. Lemons, Crit. Rev. Oral Biol. Med. 9 (1998) 449.
[27] Y. Iwasawa (Ed.), Tailored Metal Catalysts, Reidel, Dordrecht, 1986.
[28] J. Augustynski, Aspects of photo-electrochemical and surface behavior of titanium(IV) oxide, in: M.J. Clarke et al. (Eds.), Structure and Bonding 69, Springer, New York, 1988, pp. 1–61.
[29] A.F. Carley, P.R. Chalker, J.C. Riviere, M.W. Roberts, J. Chem. Soc. Faraday Trans. I 83 (1987) 351.
[30] M.W. Roberts, M. Tomellini, Catal. Today 12 (1992) 443.
[31] A.F. Carley, J.C. Roberts, M.W. Roberts, Surf. Sci. Lett. 225 (1990) L39.
[32] M. Martin, W. Mader, E. Fromm, Thin Solid Films 250 (1994) 61.
[33] I. Vaquila, M.C.G. Passeggi, J. Ferron, Phys. Rev. B 55 (1997) 13 925.
[34] W.S. Oh, C. Xu, D.Y. Kim, D.W. Goodman, J. Vac. Sci. Technol. A 15 (1997) 1710.
[35] A. Galerie, Y. Wouters, J.-P. Petit, Mater. Sci. Forum 251–254 (1997) 113.
[36] A. Azoulay, N. Shamir, V. Volterra, M.H. Mintz, Surf. Sci. 422 (1999) 141.
[37] J. Miller, S.L. Bernasek, J. Schwartz, Langmuir 10 (1994) 2629.
[38] Goodfellow customer service, personal communication.

[39] J. Miller, S.L. Bernasek, J. Schwartz, J. Am. Chem. Soc. 117 (1995) 4037.
[40] D.A. Shirley, Phys. Rev. B 5 (1972) 4709.
[41] J.F. Moulder, W.F. Stickle, P.E. Sobol, K.D. Bomben, in: J. Chastain (Ed.), Handbook of X-ray Photoelectron Spectroscopy, Perkin-Elmer, Eden Prairie, MN, 1992, pp. 72–73.
[42] S. Hofmann, Depth profiling in AES and XPS, in: D. Briggs, M.P. Seah (Eds.), Practical Surface Analysis, second ed., Vol. 1, Wiley, New York, 1994, pp. 143–194.
[43] R. Zanoni, G. Righini, A. Montenero, G. Gnappi, G. Montesperelli, E. Traversa, G. Gusmano, Surf. Interface Anal. 22 (1994) 376.
[44] J. Pouilleau, D. Devilliers, H. Groult, P.J. Marcus, Mater. Sci. 32 (1997) 5645.
[45] W.S. Epling, C.H.F. Peden, M.A. Henderson, U. Diebold, Surf. Sci. 412–413 (1998) 333.
[46] H. Idriss, K.S. Kim, M.A. Barteau, Surf. Sci. 262 (1992) 113.
[47] M.A. Henderson, W.S. Epling, C.L. Perkins, C.H.F. Peden, U.J. Diebold, Phys. Chem. B 103 (1999) 5328.
[48] G. Lu, B.E. Hayden, J. Evans, unpublished results.